NUWC-NPT Technical Report 10,709
27 July 1994

Statistics of Complex Cross Spectrum Estimate for Sinusoidal Signals and Arbitrary Noise Spectra

Albert H. Nuttall
Surface Antisubmarine Warfare Directorate

Naval Undersea Warfare Center Division
Newport, Rhode Island

PREFACE

This research was conducted under NUWC Job Order Number A10020, R&D Project Number RR00N00, **Performance Evaluation of Nonlinear Signal Processors with Mismatch**, Principal Investigator Dr. Albert H. Nuttall (Code 302). This technical report was prepared with funds provided by the NUWC In-House Independent Research Program, sponsored by the Office of Naval Research. Also, the research presented in this report was conducted under NUWC Job Order Number D15010, Project Number S0219, **AN/BQQ-5 Sonar Program**, Principal Investigator Kevin C. Collins (Code 2191), sponsored by NAVSEA, CAPT G. Kent (PMS 425).

The author of this report is located at the Naval Undersea Warfare Center Detachment, New London, CT 06320. The technical reviewer for this report was Ronald R. Kneipfer (Code 214).

Reviewed and Approved: 27 July 1994

Donald W. Counsellor
Director, Surface Antisubmarine Warfare

REPORT DOCUMENTATION PAGE

Form Approved
OMB No. 0704-0188

1. AGENCY USE ONLY (Leave blank)	2. REPORT DATE	3. REPORT TYPE AND DATES COVERED
	27 July 1994	Progress

4. TITLE AND SUBTITLE
Statistics of Complex Cross Spectrum Estimate for Sinusoidal Signals and Arbitrary Noise Spectra

5. FUNDING NUMBERS
PE 0601152N

6. AUTHOR(S)
Albert H. Nuttall

7. PERFORMING ORGANIZATION NAME(S) AND ADDRESS(ES)
Naval Undersea Warfare Center Detachment
New London, Connecticut 06320

8. PERFORMING ORGANIZATION REPORT NUMBER
NUWC-NPT TR 10,709

9. SPONSORING/MONITORING AGENCY NAME(S) AND ADDRESS(ES)
Office of Naval Research
800 North Quincy Street, BCT 1
Arlington, VA 22217-5000

10. SPONSORING/MONITORING AGENCY REPORT NUMBER

11. SUPPLEMENTARY NOTES

12a. DISTRIBUTION/AVAILABILITY STATEMENT
Approved for public release;
distribution is unlimited.

12b. DISTRIBUTION CODE

13. ABSTRACT *(Maximum 200 words)*

The joint characteristic function of the real and imaginary parts of the complex cross spectrum estimate is derived in closed form for sinusoidal signals and arbitrary noise spectra. The corresponding joint probability density function for noise-only is also obtained in closed form, while that for signal present requires a numerical procedure involving a two-dimensional fast Fourier transform. These results are used to obtain the mean and deflection of the magnitude cross spectrum estimate. Comparisons are made with the deflection of an auto spectrum estimate available from the two channels by weighted summation. Potential limitations of restricting attention to the deflection criterion as a detectability measure are pointed out.

14. SUBJECT TERMS		15. NUMBER OF PAGES
cross spectrum	spectrum estimate	58
sinusoidal signals	arbitrary noise	16. PRICE CODE
characteristic function	probability density	

17. SECURITY CLASSIFICATION OF REPORT	18. SECURITY CLASSIFICATION OF THIS PAGE	19. SECURITY CLASSIFICATION OF ABSTRACT	20. LIMITATION OF ABSTRACT
UNCLASSIFIED	UNCLASSIFIED	UNCLASSIFIED	SAR

14. SUBJECT TERMS (continued)

fast Fourie ransform
mean magni
deflection
auto spectrum estimate
Gaussian approximation
false alarm probability
detection probability

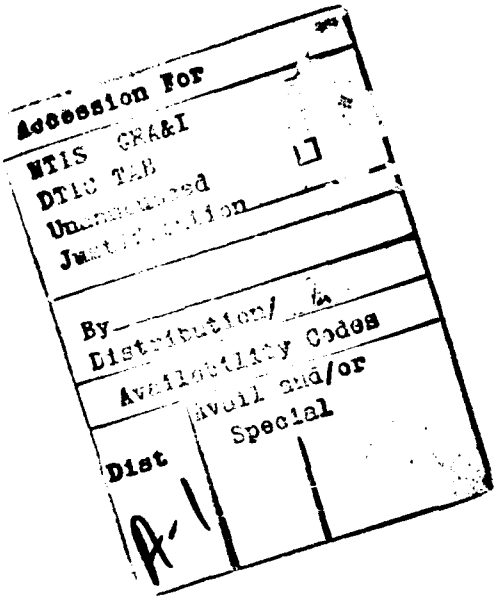

TABLE OF CONTENTS

LIST OF FIGURES

LIST OF SYMBOLS

bold	random variable
t	time, (1)
s(t)	input signal, (1)
A	amplitude of input sinewave, (1)
f_o	frequency of input sinewave, (1)
ϕ	phase of input sinewave, (1)
x(t)	input noise process in one channel
y(t)	input noise process in other channel
K	number of pieces used for spectrum estimation, (2)
w(t)	fundamental time weighting function, (2)
$w_k(t)$	k-th time weighting function, (2)
T_k	time delay of k-th time weighting function, (2)
ν	frequency variable, (3)
$W(\nu)$	fundamental spectral window, (3)
$W_k(\nu)$	k-th spectral window, (3)
f	analysis frequency of interest, (4)
S_k	k-th signal voltage density estimate, (4)
α_k, β_k	real and imaginary parts of S_k, (4)
X_k	k-th noise voltage density estimate for x(t), (5)
a_k, b_k	real and imaginary parts of X_k, (5)

Y_k	k-th noise voltage density estimate for y(t), (6)
c_k, d_k	real and imaginary parts of Y_k, (6)
G	complex cross spectrum estimate, (7)
R,Q	real and imaginary parts of G, (7)
R_k, Q_k	real and imaginary parts of k-th term, (8)
γ	nonrandom signal quantity, (9)
$R_x(\tau)$	covariance of process x(t), (10)
$G_x(\nu)$	spectrum of process x(t), (10)
σ_x^2	variance measure in x channel, (12)
$G_y(\nu)$	spectrum of process y(t), (13)
σ_y^2	variance measure in y channel, (13)
$f_k(z,y)$	joint characteristic function of R_k and Q_k, (14)
ξ, η	real arguments of joint characteristic function, (15)
z,y	auxiliary complex arguments, (15)
$f_{RQ}(z,y)$	joint characteristic function of R and Q, (19)
χ_{mn}	m,n-th joint cumulant of R and Q, (20)
R_x, R_y	signal to noise ratio measures, (22)
σ^2	variance of R and Q, (24)
p_g	Gaussian joint probability density function, (25)
μ_1	mean magnitude of G, (26)
μ_{1g}	Gaussian approximation to μ_1, (27), (28)
I_o	modified Bessel function, (28)
${}_1F_1$	confluent hypergeometric function, (28)
V	auxiliary variable, (29)
$\mu_{1g}(A=0)$	value of μ_{1g} for zero signal input, A = 0, (31)
μ_2	mean square magnitude of G, (33)

d_c	deflection of magnitude $\|G\|$, (35)
d_g	Gaussian-approximation deflection, (36)
$\mu_1(K=1)$	value of μ_1 for K = 1, (41)
$\mu_{1g}(K=1)$	value of μ_{1g} for K = 1, (42)
$d_c(K=1)$	value of d_c for K = 1, (43)
$d_g(K=1)$	value of d_g for K = 1, (44)
f_{RQ}^o	value of f_{RQ} for A = 0, (45)
B	$\sigma_x\sigma_y/K$, (45)
p_{RQ}^o	value of p_{RQ} for A = 0, (46)
$K_\nu(x)$	modified Bessel function of second kind, (46)
ρ	$(u^2 + v^2)^{\frac{1}{2}}$, (46)
$\mu_1(A=0)$	value of μ_1 for A = 0, (47)
$\mu_{2\nu}(A=0)$	2ν-th moment of $\|G\|$ for A = 0, (48)
r,q	normalized random variables, (52)
f_{rq}	joint characteristic function of r and q, (53)
p_{rq}	joint probability density function of r and q, (55)
Re	real part, (55)
ε_k	integration rule coefficient, (55)
Δ_f	sampling increment for f_{rq}, in both ξ and η, (55)
$\underline{p}_{rq}$	aliased probability density function, (55)
N	size of fast Fourier transform, (56)
f_a	collapsed version of $\varepsilon_k f_{rq}$, (56)
Δ_p	increment for $\underline{p}_{rq}$, in both u and v, (57)
D_2	double integral for moment, (58)
S	nonzero region of p_{rq}, (59)
K_m	number of samples of f_{rq} in each dimension

$z(t)$	sum process, (60)
λ	scale factor in sum, (60)
Z_k	k-th voltage density estimate of z(t), (61)
G_z	auto spectrum estimate of z(t), (62)
e_k, f_k	auxiliary random variables, (63)
σ_e^2	variance of e_k and f_k, (64)
$F_k(i\xi)$	characteristic function of k-th term of sum, (66)
$F(i\xi)$	characteristic function of G_z, (67)
χ_j	j-th cumulant of G_z, (68)
P_d	detection probability for G_z, (69)
$Pr(E)$	probability of event E, (69)
v	threshold, (69)
Q_K	Q function, (69)
P_f	false alarm probability for G_z, (70)
d_a	deflection of auto spectrum estimate G_z, (74)
d_x	deflection of random variable x, (78)
H_1	hypothesis that signal is present
H_0	hypothesis that signal is absent
m_1	mean under hypothesis H_1, (79)
Φ	error function, (79)
m_0	mean under hypothesis H_0, (80)
$\tilde{\Phi}$	inverse error function, (81)
C	dimensionless constant, (82)
y	distorted random variable, (82)
d_y	deflection of random variable y, (84)

STATISTICS OF COMPLEX CROSS SPECTRUM ESTIMATE FOR SINUSOIDAL SIGNALS AND ARBITRARY NOISE SPECTRA

INTRODUCTION

The analysis of the stability of the estimate of the complex cross spectrum usually proceeds on the basis that the two input processes have a slowly varying cross spectrum relative to the spectral window employed. See, for example, [1; (4) and sequel]. Here, we will eliminate that restriction and allow real input signals with arbitrarily narrow width, namely sinusoids, and allow real additive input noises with arbitrary spectra.

On the other hand, we will restrict consideration to the special case where the two input noise processes are zero mean Gaussian and are statistically independent of each other. Furthermore, the temporal weightings applied will be presumed nonoverlapping in time, thereby leading to (approximately) independent spectral estimates for each time segment.

We will derive the exact joint characteristic function of the real and imaginary parts R and Q, of the cross spectrum estimate $G = R + iQ$, with both signal and noise present. This result enables determination of the high-order joint cumulants of random variables R and Q, for arbitrary signal-to-noise ratios.

For the noise-only case, the corresponding joint probability density function of random variables R and Q will be derived in closed form. It can then be used to derive various moments of the magnitude of estimate G, such as the average magnitude $\overline{|G|}$.

When signal is present, the joint probability density function of R and Q cannot be found in closed form. Instead, a two-dimensional fast Fourier transform is utilized, followed by numerical integration to find the moments of interest. Comparison of these accurate results with a Gaussian approximation affords quantitative verification of the Gaussian approximation when the number of pieces, K, used in the finite average for cross spectrum estimate G exceeds 10 approximately.

A deflection criterion of cross spectrum magnitude estimate |G| is defined and evaluated, both numerically and by use of the same Gaussian approximation for the joint probability density function of R and Q. Finally, the same statistics are evaluated for an auto spectrum estimate obtained from the two input processes optimally scaled prior to addition.

PROBLEM DEFINITION

This study is a follow-on to an earlier report [1], where the overlapped fast Fourier transform processing method of weighted data segments for the purpose of estimation of the cross spectrum was well documented. Familiarity with that material and results is presumed in the following development.

A common sinusoidal signal $s(t)$ at frequency f_o is present in both input channels; that is,

$$s(t) = A \cos(2\pi f_o t + \phi) \ , \tag{1}$$

where ϕ is a random variable uniformly distributed over 2π. The input noise processes in the two channels are $x(t)$ and $y(t)$, respectively. The k-th time weighting function and its spectral window (Fourier transform) are given by

$$w_k(t) = w(t - T_k) \quad \text{for } 1 \le k \le K \ , \tag{2}$$

$$W_k(\nu) \equiv \int dt \, \exp(-i2\pi\nu t) \, w_k(t) = \exp(-i2\pi\nu T_k) \, W(\nu) \ , \tag{3}$$

where K is the total number of pieces used in the cross spectrum estimate G, and $W(\nu)$ is the window (Fourier transform) corresponding to fundamental time weighting $w(t)$. Time delays $\{T_k\}$ are taken widely enough spaced that individual temporal weightings $\{w_k(t)\}$ do not overlap on the time axis. (Integrals without limits are over the range of nonzero integrand.)

The k-th voltage density estimate, at analysis frequency f, of the signal component is, for both channels,

$$S_k \equiv \int dt\ \exp(-i2\pi ft)\ w_k(t)\ A\ \cos(2\pi f_o t + \phi) = \qquad (4)$$

$$\approx \frac{A}{2}\ e^{i\phi} \int dt\ w_k(t)\ \exp(-i2\pi(f-f_o)t) = \frac{A}{2}\ e^{i\phi}\ W_k(f-f_o) \equiv \alpha_k + i\beta_k\ ,$$

where random variables α_k and β_k are real. It is presumed that analysis frequency f is close to the actual input signal center frequency f_o, but they need not be equal.

The k-th voltage density estimate, at analysis frequency f, of the noise component x(t) is

$$X_k \equiv \int dt\ \exp(-i2\pi ft)\ w_k(t)\ x(t) \equiv a_k + ib_k\ , \qquad (5)$$

for $1 \le k \le K$. Random variables a_k and b_k are zero mean Gaussian, since the two input processes x(t) and y(t) are zero mean Gaussian processes. The corresponding quantities for the other channel are

$$Y_k \equiv \int dt\ \exp(-i2\pi ft)\ w_k(t)\ y(t) \equiv c_k + id_k\ . \qquad (6)$$

The complex cross spectrum estimate at analysis frequency f is therefore given by

$$G \equiv \frac{1}{K} \sum_{k=1}^{K} (S_k + X_k)(S_k + Y_k)^* =$$

$$= \frac{1}{K} \sum_{k=1}^{K} (\alpha_k + i\beta_k + a_k + ib_k)\ (\alpha_k - i\beta_k + c_k - id_k) =$$

$$= \frac{1}{K} \sum_{k=1}^{K} (R_k + iQ_k) \equiv R + iQ\ , \qquad (7)$$

where real and imaginary parts

$$R_k = (\alpha_k + a_k)(\alpha_k + c_k) + (\beta_k + b_k)(\beta_k + d_k) \ ,$$

$$Q_k = (\beta_k + b_k)(\alpha_k + c_k) - (\alpha_k + a_k)(\beta_k + d_k) \ . \qquad (8)$$

It is important to notice from (4) and (3) that

$$|S_k|^2 = |\alpha_k + i\beta_k|^2 = \alpha_k^2 + \beta_k^2 = \tfrac{1}{4} A^2 \ |W(f-f_o)|^2 \equiv \gamma \ , \qquad (9)$$

where the latter quantity γ is a constant, not a random variable, and that, furthermore, γ is independent of k, the segment number.

STATISTICS OF a_k AND b_k

From (5), we observe that ensemble average

$$\overline{|X_k|^2} = \overline{|a_k + ib_k|^2} = \overline{a_k^2} + \overline{b_k^2} =$$

$$= \iint dt\, du\, \exp(-i2\pi f(t-u))\ w_k(t)\ w_k^*(u)\ R_x(t-u) =$$

$$= \int d\nu\ G_x(\nu)\ |W_k(f-\nu)|^2 = \int d\nu\ G_x(\nu)\ |W(f-\nu)|^2 \ , \qquad (10)$$

where $R_x(\tau)$ and $G_x(\nu)$ are, respectively, the covariance and spectrum of random process $x(t)$, and we used (3). Again, notice that this average is independent of k. Also, the result in (10) holds regardless of the relative widths and variations of window $|W(\nu)|^2$ and spectrum $G_x(\nu)$.

At the same time, from (5) and (3),

$$\overline{X_k^2} = \overline{(a_k + ib_k)^2} = \overline{a_k^2} - \overline{b_k^2} + i2\,\overline{a_k\,b_k} =$$

$$= \int d\nu\; G_x(\nu)\; W_k(f-\nu)\; W_k(f+\nu) =$$

$$= \exp(-i4\pi f T_k) \int d\nu\; G_x(\nu)\; W(f-\nu)\; W(f+\nu) \cong 0\ , \qquad (11)$$

if analysis frequency f is not near zero frequency. Combining (10) and (11), we find properties

$$\overline{a_k^2} = \overline{b_k^2} = \tfrac{1}{2} \int d\nu\; G_x(\nu)\; |W(f-\nu)|^2 \equiv \sigma_x^2\ , \quad \overline{a_k\,b_k} = 0\ , \qquad (12)$$

which are independent of k. Thus, Gaussian random variables a_k and b_k are statistically independent of each other.

STATISTICS OF c_k AND d_k

In an entirely similar fashion, but working instead from (6),

$$\overline{c_k} = \overline{d_k} = 0\ , \quad \overline{c_k\,d_k} = 0\ ,$$

$$\overline{c_k^2} = \overline{d_k^2} = \tfrac{1}{2} \int d\nu\; G_y(\nu)\; |W(f-\nu)|^2 \equiv \sigma_y^2\ , \qquad (13)$$

all quantities being independent of k. Furthermore, the time delays $\{T_k\}$ in (2) are widely enough separated that all the random variables for weighting k are independent of all those for weighting m, when $k \neq m$.

JOINT CHARACTERISTIC FUNCTION OF R AND Q

The joint characteristic function of the k-th pair of random variables R_k and Q_k in (7) and (8) is given by ensemble average

$$f_k(z,y) \equiv \overline{\exp(zR_k + yQ_k)} = \overline{\exp\Big[z(\alpha_k+a_k)(\alpha_k+c_k) + \cdots}$$

$$\overline{\cdots + z(\beta_k+b_k)(\beta_k+d_k) + y(\beta_k+b_k)(\alpha_k+c_k) - y(\alpha_k+a_k)(\beta_k+d} \quad , \tag{14}$$

where we have let variables

$$z = i\xi \quad \text{and} \quad y = i\eta, \quad \xi \text{ and } \eta \text{ real} \ , \tag{15}$$

for shorthand purposes. At the same time, from (12) and (13), the joint probability density function of a_k, b_k, c_k, d_k is, for all k, given by

$$p(a,b,c,d) = \left(2\pi\sigma_x^2\right)^{-1} \left(2\pi\sigma_y^2\right)^{-1} \exp\left(-\frac{a^2+b^2}{2\sigma_x^2} - \frac{c^2+d^2}{2\sigma_y^2}\right) . \tag{16}$$

When we employ this result for p in the average required by (14), holding random variables α_k and β_k fixed for now, the resulting four-fold integral can be evaluated by first evaluating the double integral on a and b, followed by the double integral on c and d, by means of the following result:

$$\iint dx\, dy\, \exp\left(-\tfrac{1}{2}\alpha x^2 - \tfrac{1}{2}\beta y^2 + \gamma xy + \mu x + \nu y\right) =$$

$$= 2\pi \left(\alpha\beta-\gamma^2\right)^{-\frac{1}{2}} \exp\left(\frac{\beta\mu^2 + \alpha\nu^2 + 2\gamma\mu\nu}{2(\alpha\beta-\gamma^2)}\right) \tag{17}$$

for $\alpha_r > 0$, $\beta_r > 0$, $\alpha_r \beta_r > \gamma_r^2$. The end result, after much

manipulation, is the joint characteristic function of R_k and Q_k, conditioned on given fixed values of random variables α_k and β_k, namely

$$f_k(z,y) = \frac{1}{1 - \sigma_x^2 \sigma_y^2 (z^2 + y^2)} \exp\left[\gamma \frac{z + (z^2 + y^2)(\sigma_x^2 + \sigma_y^2)/2}{1 - \sigma_x^2 \sigma_y^2 (z^2 + y^2)}\right] \quad (18)$$

where we used relation (9).

But, since (18) contains no random variables, it is actually the unconditional joint characteristic function of R_k and Q_k. Also, since the constant γ is independent of k, we see that $f_k(z,y)$ is independent of k. This leads to the desired result, namely the joint characteristic function of summation variables R and Q in (7), as

$$f_{RQ}(z,y) = \overline{\exp(zR + yQ)} = \overline{\exp\left(\frac{z}{K}\sum_{k=1}^{K} R_k + \frac{y}{K}\sum_{k=1}^{K} Q_k\right)} =$$

$$= \prod_{k=1}^{K} f_k\left(\frac{z}{K}, \frac{y}{K}\right) = f_1\left(\frac{z}{K}, \frac{y}{K}\right)^K =$$

$$= \left[1 - \sigma_x^2 \sigma_y^2 (z^2 + y^2)/K^2\right]^{-K} \exp\left[\gamma \frac{z + (z^2 + y^2)(\sigma_x^2 + \sigma_y^2)/(2K)}{1 - \sigma_x^2 \sigma_y^2 (z^2 + y^2)/K^2}\right] . \quad (19)$$

This is an exact result for the joint characteristic function of R and Q, under the conditions cited above, such as disjoint temporal weightings $\{w_k(t)\}$, common sinusoidal signal s(t), and independent input noise processes x(t) and y(t). The complex cross spectrum estimate is given by (7) as G = R + iQ.

JOINT CUMULANTS OF R AND Q

When we expand ln $f_{RQ}(z,y)$ in (19) in a power series in z and y according to

$$\ln f_{RQ}(z,y) = \sum_{m=0}^{\infty} \sum_{n=0}^{\infty} \chi_{mn} \frac{z^m}{m!} \frac{y^n}{n!} , \quad \chi_{oo} = 0 , \tag{20}$$

then, χ_{mn} is the m,n-th joint cumulant of R and Q. There follows

$$\chi_{10} = \gamma , \quad \chi_{01} = 0 , \quad \chi_{mn} = 0 \quad \text{for } m + n = 3,5,7,...$$

$$\chi_{20} = \chi_{02} = \frac{2\,\sigma_x^2\,\sigma_y^2}{K} (1 + R_x + R_y) , \quad \chi_{11} = 0 ,$$

$$\chi_{22} = \frac{4\,\sigma_x^4\,\sigma_y^4}{K^3} (1 + 2R_x + 2R_y) ,$$

$$\chi_{40} = \chi_{04} = 3\,\chi_{22} , \quad \chi_{31} = \chi_{13} = 0 , \tag{21}$$

where we have defined, with the help of (9) and (12),

$$R_x = \frac{\gamma}{2\sigma_x^2} = \frac{\frac{1}{4} A^2 \, |W(f-f_o)|^2}{\int d\nu \; G_x(\nu) \; |W(f-\nu)|^2} ,$$

$$R_y = \frac{\gamma}{2\sigma_y^2} = \frac{\frac{1}{4} A^2 \, |W(f-f_o)|^2}{\int d\nu \; G_y(\nu) \; |W(f-\nu)|^2} . \tag{22}$$

These latter quantities are measures of the signal-to-noise power ratios at the outputs of window $|W(\nu)|^2$ in (3).

The results in (21) indicate that as the number of pieces $K \to \infty$, the two random variables R and Q tend to joint Gaussian. For example, we find

$$\frac{\chi_{40}}{\chi_{20}^2} = \frac{3}{K} \frac{1 + 2R_x + 2R_y}{(1 + R_x + R_y)^2} \to 0 \text{ as } K \to \infty . \qquad (23)$$

Since the joint third-order moments are all zero, this result indicates a rather rapid approach to the Gaussian approximation.

GAUSSIAN APPROXIMATION

The quantities χ_{10} and χ_{01} in (21) are the means of R and Q, respectively. Also, χ_{20} and χ_{02} are the respective variances, which are equal and will be denoted by σ^2; that is,

$$\sigma^2 = \frac{2\,\sigma_x^2\,\sigma_y^2}{K}\,(1 + R_x + R_y)\ . \tag{24}$$

Since covariance χ_{11} is zero, the Gaussian approximation to the two-dimensional probability density function of R and Q is given by

$$p_g(u,v) \equiv \frac{1}{2\pi\sigma^2}\exp\left(-\frac{(u-\gamma)^2 + v^2}{2\sigma^2}\right) \quad \text{for all } u,v\ . \tag{25}$$

MEAN MAGNITUDE OF G

With this approximation at hand, we can now evaluate some moments of G that are not available directly from joint characteristic function (19) or joint cumulants (21). In particular, we are interested in the mean magnitude of complex cross spectrum estimate G = R + iQ; namely,

$$\mu_1 \equiv \overline{|G|} = \overline{(R^2 + Q^2)^{\frac{1}{2}}} = \iint du\,dv\,(u^2 + v^2)^{\frac{1}{2}}\,p_{RQ}(u,v) = \tag{26}$$

$$\approx \iint du\,dv\,(u^2 + v^2)^{\frac{1}{2}}\,p_g(u,v) \equiv \mu_{1g} = \tag{27}$$

$$= \iint du\, dv\, \frac{(u^2 + v^2)^{\frac{1}{2}}}{2\pi\sigma^2} \exp\left(- \frac{(u - \gamma)^2 + v^2}{2\sigma^2}\right) =$$

$$= \int_0^{\infty} dr\, r \int_{-\pi}^{\pi} d\theta\, \frac{r}{2\pi\sigma^2} \exp\left(- \frac{r^2 - 2\gamma r \cos\theta + \gamma^2}{2\sigma^2}\right) =$$

$$= \int_0^{\infty} dr\, \frac{r^2}{\sigma^2} \exp\left(- \frac{r^2 + \gamma^2}{2\sigma^2}\right) I_0\left(\frac{\gamma r}{\sigma^2}\right) =$$

$$= \left(\frac{\pi}{2}\right)^{\frac{1}{2}} \sigma \exp(-V)\ {}_1F_1(1.5;1;V) = \left(\frac{\pi}{2}\right)^{\frac{1}{2}} \sigma\ {}_1F_1(-.5;1;-V)\ , \qquad (28)$$

where we used [2; 6.631 1], [3; 13.1.27], and defined

$$V = \frac{\gamma^2}{2\sigma^2} = K \frac{R_x R_y}{1 + R_x + R_y}\ . \qquad (29)$$

The function ${}_1F_1$ is the confluent hypergeometric function [3; 13.1.2 and 13.1.10].

It must be repeated that (28) is an approximation for the desired average μ_1, because the Gaussian density function $p_g(u,v)$, employed in (27) and the sequel, is itself an approximation to the true (unknown) probability density function $p_{RQ}(u,v)$ of R and Q. The result of the Gaussian approximation in (27) and (28) has been denoted by μ_{1g}.

Upon use of (24), the mean value approximation, μ_{1g} in (28), takes the form

$$\mu_{1g} = \sigma_x\, \sigma_y \left(\frac{\pi}{K}\right)^{\frac{1}{2}} (1 + R_x + R_y)^{\frac{1}{2}}\ {}_1F_1(-.5;1;-V)\ , \qquad (30)$$

where the various parameters are defined in (12), (13), (22), and (29). If the signal is absent at the input, then A = 0, $R_x = 0$, $R_y = 0$, V = 0, giving

$$\mu_{1g}(A=0) = \sigma_x \, \sigma_y \left(\frac{\pi}{K}\right)^{\frac{1}{2}}, \tag{31}$$

which decays to 0 as $K^{-\frac{1}{2}}$ for large K.

On the other hand, for A > 0, suppose that K is large enough that parameter V in (29) is large compared with 1. Then, we have the asymptotic result [4; A.1.16b]

$$\mu_{1g} \sim \gamma\left(1 + \frac{1}{4V}\right) = \frac{1}{4} A^2 \, |W(f-f_o)|^2 \left(1 + \frac{1}{4V}\right) \quad \text{as } V \to \infty , \tag{32}$$

where we used (9). That is, the mean magnitude μ_{1g} approaches the signal-only output γ, with an additive term that decays as K^{-1}, not $K^{-\frac{1}{2}}$ as in (31). These results are expected to be most accurate for large K, where the Gaussian approximation is best.

MEAN SQUARE MAGNITUDE OF G

The mean square magnitude of cross spectrum estimate G is

$$\mu_2 \equiv \overline{|G|^2} = \overline{R^2} + \overline{Q^2} = \overline{R}^2 + \sigma_R^2 + \overline{Q}^2 + \sigma_Q^2 = \gamma^2 + 2\sigma^2 , \tag{33}$$

where we used (21) and (24). Upon additional use of (22), this develops into

$$\mu_2 = 4 \, \sigma_x^2 \, \sigma_y^2 \left(R_x \, R_y + \frac{1 + R_x + R_y}{K}\right) . \tag{34}$$

This result is exact, having been developed directly from the exact joint characteristic function (19) of R and Q; hence, there is no need to add subscript g to μ_2. However, it can be noted that use of the Gaussian probability density approximation (25) yields exactly the same result (34).

DEFLECTION OF MAGNITUDE |G|

The deflection of the magnitude of the complex cross spectrum estimate |G| is defined here as

$$d_c \equiv \frac{\mu_1 - \mu_1(A=0)}{\left(\mu_2(A=0) - \mu_1^2(A=0)\right)^{\frac{1}{2}}} \, . \tag{35}$$

However, since only the approximate result μ_{1g} is available, we also define the Gaussian-approximation deflection as

$$d_g \equiv \frac{\mu_{1g} - \mu_{1g}(A=0)}{\left(\mu_2(A=0) - \mu_{1g}^2(A=0)\right)^{\frac{1}{2}}} \, . \tag{36}$$

Substitution of (30), (31), and (34) (with A = 0) yields

$$d_g = \left(\frac{\pi}{4-\pi}\right)^{\frac{1}{2}} \left[(1 + R_x + R_y)^{\frac{1}{2}} \, {}_1F_1(-.5;1;-V) - 1\right] , \tag{37}$$

where V is given by (29).

If the number of pieces K is so large that V >> 1, use of the asymptotic behavior of ${}_1F_1$ [4; A.1.16b] yields

$$d_g \sim \left(\frac{4}{4-\pi} K R_x R_y\right)^{\frac{1}{2}} - \left(\frac{\pi}{4-\pi}\right)^{\frac{1}{2}} = 2.16 (K R_x R_y)^{\frac{1}{2}} - 1.91 \quad \text{as } K \to \infty . \tag{38}$$

Thus, the Gaussian deflection increases as $K^{\frac{1}{2}}$ for large K and is proportional to the geometric mean of the individual signal-to-noise ratios.

A comparison of the Gaussian deflection d_g in (37) with some exact results for the desired deflection d_c in (35) will be made in the next section for selected values of K and A. The asymptotic behavior (38) will not be employed for that comparison, since it is valid only for larger values of K.

EXACT RESULTS

Some special cases for mean magnitude μ_1 defined in (26) can be carried out in closed form. These results complement the earlier approximations, furnish a check on the Gaussian approximations, and establish their regions of accuracy.

MEAN MAGNITUDE FOR ONE PIECE, K = 1

When K = 1, the magnitude of complex estimate G follows immediately from (7) as

$$|G| = \left[(\alpha_1+a_1)^2 + (\beta_1+b_1)^2\right]^{\frac{1}{2}} \left[(\alpha_1+c_1)^2 + (\beta_1+d_1)^2\right]^{\frac{1}{2}} . \qquad (39)$$

The desired average over the six random variables involved is conducted by first holding random variables α_1 and β_1 fixed. The conditional average over the remaining four random variables then factors into the product of two averages. The first conditional average can be expressed as

$$\overline{\left[(\alpha_1+a_1)^2 + (\beta_1+b_1)^2\right]^{\frac{1}{2}}} =$$

$$= \iint \frac{da\ db}{2\pi\sigma_x^2} \exp\left[-\frac{a^2+b^2}{2\sigma_x^2}\right] \left[(\alpha_1+a)^2 + (\beta_1+b)^2\right]^{\frac{1}{2}} =$$

$$= \iint \frac{dt\ du}{2\pi\sigma_x^2} \exp\left[-\frac{(t-\alpha_1)^2 + (u-\beta_1)^2}{2\sigma_x^2}\right] (t^2+u^2)^{\frac{1}{2}} =$$

$$= \int_0^{\infty} dr\ r \int_{-\pi}^{\pi} d\theta\ \frac{r}{2\pi\sigma_x^2} \exp\left(-\frac{r^2 - 2\alpha_1 r\cos\theta - 2\beta_1 r\sin\theta + \alpha_1^2 + \beta_1^2}{2\sigma_x^2}\right) =$$

$$= \int_0^{\infty} dr\ \frac{r^2}{\sigma_x^2} \exp\left(-\frac{r^2+\gamma}{2\sigma_x^2}\right) I_o\left(\frac{\gamma^{\frac{1}{2}} r}{\sigma_x^2}\right) = \left(\frac{\pi}{2}\right)^{\frac{1}{2}} \sigma_x\ {}_1F_1(-.5;1;-R_x)\ , \quad (40)$$

where we used (16), (9), [2; 6.631 1, 9.210 1, 9.212 1], and (22). But, it must now be observed that no random variables remain in the end result, meaning that no further averaging is required! A similar approach can be used for the second term in (39), yielding the desired exact result for the mean of |G| as

$$\mu_1(K=1) = \frac{\pi}{2}\ \sigma_x\ \sigma_y\ {}_1F_1(-.5;1;-R_x)\ {}_1F_1(-.5;1;-R_y)\ . \quad (41)$$

This can be compared with the corresponding Gaussian approximation according to (30) and (29), namely

$$\mu_{1g}(K=1) = \pi^{\frac{1}{2}}\ \sigma_x\ \sigma_y\ (1+R_x+R_y)^{\frac{1}{2}}\ {}_1F_1\left(-.5;1;-\frac{R_x\ R_y}{1+R_x+R_y}\right)\ . \quad (42)$$

A short table follows; for K = 1, the Gaussian approximation is anywhere from 6% to 13% in error, over this range of values.

Tabulation of Mean Magnitude for K = 1

R_x	R_y	$\frac{\mu_1(K=1)}{\sigma_x\ \sigma_y}$	$\frac{\mu_{1g}(K=1)}{\sigma_x\ \sigma_y}$	$\frac{\mu_{1g}(K=1)}{\mu_1(K=1)}$
0	0	1.57	1.77	1.13
.5	.25	2.18	2.43	1.12
.5	.5	2.40	2.66	1.11
1	.25	2.55	2.80	1.10
1	.5	2.81	3.08	1.10
1	1	3.29	3.56	1.08
2	.5	3.52	3.77	1.07
2	1	4.12	4.38	1.06

DEFLECTION FOR ONE PIECE, K = 1

The deflection of interest was defined in (35). When we use exact results (41) and (34), we find, that for K = 1,

$$d_c(K=1) = \frac{\pi}{(16 - \pi^2)^{\frac{1}{2}}} \left[{}_1F_1(-.5;1;-R_x)\ {}_1F_1(-.5;1;-R_y) - 1 \right] . \quad (43)$$

On the other hand, the Gaussian approximation to the deflection is given by (37) and (29) in the form

$$d_g(K=1) = \left(\frac{\pi}{4-\pi}\right)^{\frac{1}{2}} \left[(1+R_x+R_y)^{\frac{1}{2}}\ {}_1F_1\left(-.5;1;-\frac{R_x R_y}{1+R_x+R_y}\right) - 1 \right] . \quad (44)$$

A comparison of these two results is given in the following table; the Gaussian approximation overestimates the deflection by about 40% for K = 1. This is not too surprising when we recall that the Gaussian approximation cannot be expected to be valid for K = 1, but rather to be best for large K, where summation variables R and Q in (7) are tending toward Gaussian.

Tabulation of Deflection for K = 1

R_x	R_y	$d_c(K=1)$	$d_g(K=1)$	$\frac{d_g(K=1)}{d_c(K=1)}$
0	0	0+	0+	1.51
.5	.25	.489	.707	1.45
.5	.5	.668	.959	1.43
1	.25	.789	1.11	1.41
1	.5	.999	1.41	1.41
1	1	1.39	1.93	1.39
2	.5	1.57	2.16	1.37
2	1	2.06	2.81	1.37

JOINT PROBABILITY DENSITY FUNCTION FOR SIGNAL ABSENT, ANY K

When amplitude A in input signal (1) is zero, then parameter γ in (9) is zero, and the exact joint characteristic function of R and Q in (19) reduces to

$$f^{o}_{RQ}(i\xi, i\eta) \equiv \left[1 + B^2(\xi^2 + \eta^2)\right]^{-K} , \tag{45}$$

where we used (15) and defined $B = \sigma_x\sigma_y/K$. The corresponding exact joint probability density function of R and Q is then

$$p^{o}_{RQ}(u,v) = \frac{1}{4\pi^2} \iint d\xi\, d\eta\, \exp(-iu\xi - iv\eta) \left[1 + B^2(\xi^2 + \eta^2)\right]^{-K} =$$

$$= \frac{1}{4\pi^2} \int_0^{\infty} dr\, r \int_{-\pi}^{\pi} d\theta\, \frac{\exp[-ir(u\cos\theta + v\sin\theta)]}{\left(1 + B^2r^2\right)^K} =$$

$$= \frac{1}{2\pi} \int_0^{\infty} dr\, r\, \frac{J_o(\rho r)}{\left(1 + B^2r^2\right)^K} = \frac{\rho^{K-1}}{\pi\, 2^K\, (K-1)!\, B^{K+1}}\, K_{K-1}\left(\frac{\rho}{B}\right) , \tag{46}$$

where we have defined $\rho = (u^2 + v^2)^{\frac{1}{2}}$ and used [2; 6.565 4]. The function $K_\nu(x)$ is a modified Bessel function of the second kind and order ν [3; 9.6]. Relation (46), which applies only for signal amplitude A = 0, is valid for all argument values u,v and any number of pieces K; this joint density is seen to be a function only of radius $(u^2 + v^2)^{\frac{1}{2}}$.

MOMENTS OF MAGNITUDE ESTIMATE |G| FOR SIGNAL ABSENT, ANY K

The exact mean magnitude $\mu_1 = \overline{|G|}$ is given by (26). When signal amplitude A = 0, this becomes

$$\mu_1(A=0) = \iint du\, dv\, (u^2 + v^2)^{\frac{1}{2}}\, p^o_{RQ}(u,v) =$$

$$= \int_0^\infty d\rho\, \rho \int_{-\pi}^{\pi} d\phi\, \rho\, \frac{\rho^{K-1}}{\pi\, 2^K\, (K-1)!\, B^{K+1}}\, K_{K-1}\left(\frac{\rho}{B}\right) =$$

$$= \pi^{\frac{1}{2}}\, B\, \frac{\Gamma(K+.5)}{\Gamma(K)} = \sigma_x\, \sigma_y\, \pi\, \frac{(1/2)_K}{(1)_K} \quad \text{for all K ,} \tag{47}$$

where we used (46), [2; 6.561 16], and $B = \sigma_x\sigma_y/K$. More generally, the 2ν-th moment of |G| for signal absent is available according to

$$\mu_{2\nu}(A=0) = \iint du\, dv\, (u^2+v^2)^\nu\, p^o_{RQ}(u,v) = \frac{\Gamma(K+\nu)\ \Gamma(\nu+1)}{\Gamma(K)} \left(\frac{2\sigma_x\sigma_y}{K}\right)^{2\nu} \tag{48}$$

which is exact for all K and ν. As checks on (48), we have: 1 for ν = 0; result (47) for ν = ½; and $4\ \sigma_x^2\ \sigma_y^2/K$ for ν = 1. The last result is the mean square value $\overline{R^2} + \overline{Q^2}$ and agrees with exact result (34) when signal amplitude A = 0 there. The asymptotic behavior of moment (48) is given by

$$\mu_{2\nu}(A=0) \sim \Gamma(\nu+1) \left(\frac{4\ \sigma_x^2\ \sigma_y^2}{K}\right)^\nu \quad \text{as } K \to \infty\ , \tag{49}$$

where we used [3; 6.1.47].

The Gaussian approximation, $\mu_{1g}(A=0)$, to $\mu_1(A=0)$ is given by (31). A comparison of the two is given below; it reveals that the Gaussian approximation is excellent for $K > 10$.

Tabulation of Mean Magnitude for A = 0

K	$\mu_1(A=0)/(\sigma_x\sigma_y)$	$\mu_{1g}(A=0)/(\sigma_x\sigma_y)$
1	1.5708	1.7725
2	1.1781	1.2533
3	.9817	1.0233
4	.8590	.8862
5	.7731	.7927
6	.7087	.7236
7	.6581	.6699
8	.6169	.6267
9	.5827	.5908
10	.5535	.5605
20	.3939	.3963
30	.3223	.3236
40	.2794	.2802
50	.2500	.2507
60	.2283	.2288
70	.2115	.2118
80	.1979	.1982
90	.1866	.1868
100	.1770	.1772

JOINT PROBABILITY DENSITY FUNCTION FOR SIGNAL PRESENT, ANY K

We have analytically determined the exact joint characteristic function of R and Q in (19), for arbitrary signal amplitude A and number of pieces K. However, the corresponding joint probability density function $p_{RQ}(u,v)$ is not generally available in closed form. When (19) is substituted into the double Fourier transform for $p_{RQ}(u,v)$, and a change to polar coordinates is made, the following single integral results:

$$p_{RQ}(u,v) = \frac{1}{2\pi} \int_0^\infty \frac{dr\ r}{B(r)^K} \exp\left[\frac{-\gamma\left(\sigma_x^2+\sigma_y^2\right)r^2}{2K\ B(r)}\right] J_o(D(r;u,v)) \ , \quad (50)$$

where

$$B(r) = 1 + \frac{\sigma_x^2\ \sigma_y^2\ r^2}{K^2} \ , \quad D(r;u,v) = r\left[\left(u - \frac{\gamma}{B(r)}\right)^2 + v^2\right]^{\frac{1}{2}} . \quad (51)$$

Although numerical values could be obtained from (50), a more efficient approach is to use a two-dimensional fast Fourier transform directly on characteristic function (19).

We begin by defining, for numerical convenience, the normalized random variables

$$r = \frac{R}{\sigma_x\ \sigma_y} \ , \quad q = \frac{Q}{\sigma_x\ \sigma_y} \ . \quad (52)$$

The joint characteristic function of r and q is then

$$f_{rq}(i\xi,i\eta) \equiv \overline{\exp(i\xi r+i\eta q)} = \overline{\exp\left(\frac{i\xi R+i\eta Q}{\sigma_x\ \sigma_y}\right)} = f_{RQ}\left(\frac{i\xi}{\sigma_x\sigma_y},\frac{i\eta}{\sigma_x\sigma_y}\right) =$$

$$= \left[1 + (\xi^2+\eta^2)/K^2\right]^{-K} \exp\left(\frac{i\xi 2R_x^{\frac{1}{2}}R_y^{\frac{1}{2}} - (\xi^2+\eta^2)(R_x+R_y)/K}{1 + (\xi^2+\eta^2)/K^2}\right) , \quad (53)$$

where we used (19) and (22). There follows

$$\bar{r} = 2\ R_x^{\frac{1}{2}}\ R_y^{\frac{1}{2}} , \quad \bar{q} = 0 , \quad \overline{r\ q} = 0 , \quad \sigma_r^2 = \sigma_q^2 = 2(1+R_x+R_y)/K . \quad (54)$$

The joint probability density function of r and q is

$$p_{rq}(u,v) = \frac{1}{4\pi^2} \iint d\xi\ d\eta\ \exp(-iu\xi-iv\eta)\ f_{rq}(i\xi,i\eta) =$$

$$= \frac{1}{2\pi^2}\ \mathrm{Re} \int_0^{\infty} d\xi \int_{-\infty}^{\infty} d\eta\ \exp(-iu\xi-iv\eta)\ f_{rq}(i\xi,i\eta) =$$

$$\approx \frac{\Delta_f^2}{2\pi^2}\ \mathrm{Re} \sum_{k=0}^{\infty}{}' \varepsilon_k \sum_{\ell=-\infty}^{\infty} \exp\left(-i\Delta_f(uk+v\ell)\right)\ f_{rq}\left(ik\Delta_f,i\ell\Delta_f\right) , \quad (55)$$

where we used the conjugate symmetry of f_{rq}, and took a common sampling increment Δ_f for f_{rq}, in both ξ and η. Coefficient ε_k is associated with the trapezoidal rule and is 1 for all k except for $\varepsilon_o = 1/2$. It should be observed that the resulting approximation in (55), which will be denoted by $p_{rq}(u,v)$, is periodic in both u and v, with period $2\pi/\Delta_f$. This aliased probability density function, $p_{rq}(u,v)$, is the quantity that will be evaluated.

We now take samples of the function $p_{rq}(u,v)$ over full periods in u and v, that is, $0 \le m,n \le N-1$, according to

$$p_{rq}\left(\frac{2\pi m}{N\Delta_f},\frac{2\pi n}{N\Delta_f}\right) = \frac{\Delta_f^2}{2\pi^2}\,\mathrm{Re}\sum_{k=0}^{\infty}\varepsilon_k\sum_{\ell=-\infty}^{\infty}\exp\left(\frac{-i2\pi}{N}(mk+n\ell)\right)\,f_{rq}(ik\Delta_f,i\ell\Delta_f)$$

$$= \frac{\Delta_f^2}{2\pi^2}\,\mathrm{Re}\sum_{k=0}^{N-1}\sum_{\ell=0}^{N-1}\exp\left(\frac{-i2\pi}{N}(mk+n\ell)\right)\,f_a(ik\Delta_f,i\ell\Delta_f)\ , \qquad (56)$$

where $\{f_a(ik\Delta_f,i\ell\Delta_f)\}$ is the collapsed (or prealiased) version of $\{\varepsilon_k\, f_{rq}(ik\Delta_f,i\ell\Delta_f)\}$. No approximation is involved in the last step in (56), in reducing the infinite sums to finite sums. The double sum in (56) will be recognized as a two-dimensional fast Fourier transform, when N is taken as a power of 2.

The common increment in the two arguments of the aliased probability density function $p_{rq}(u,v)$ in (56) is

$$\Delta_p = \frac{2\pi}{N\Delta_f}\ . \qquad (57)$$

Sampling increment Δ_f in ξ and η must be small enough that the resulting aliasing in periodic function $p_{rq}(u,v)$ is insignificant. Also, sampling increment Δ_p in u and v must be small enough to track important variations in $p_{rq}(u,v)$. This will generally require large values of N.

MEAN MAGNITUDE FOR SIGNAL PRESENT, ANY K

The desired moment is mean magnitude

$$\mu_1 = \overline{(R^2 + Q^2)^{\frac{1}{2}}} = \sigma_x \sigma_y \overline{(r^2 + q^2)^{\frac{1}{2}}} =$$

$$= \sigma_x \sigma_y \iint du\, dv\, (u^2 + v^2)^{\frac{1}{2}} p_{rq}(u,v) \equiv \sigma_x \sigma_y D_2 . \qquad (58)$$

In order to evaluate double integral D_2, three approximations must be accepted. First, the doubly infinite range must be replaced by a square of size $2\pi/\Delta_f$ covering the region where $p_{rq}(u,v)$ is essentially nonzero; this region, to be denoted by S, is roughly centered at $u,v = \bar{r},\bar{q}$. Then, $p_{rq}(u,v)$ must be replaced by $p_{rq}(u,v)$, since the former function cannot be evaluated. Finally, the double integral must be replaced by a double sum, using the sample points furnished by (56). The accuracy of these three replacements depends critically on the ability to accomplish the goals listed under (57), and therefore on the ability to utilize large values of N in (56). The resulting approximation to D_2 is

$$D_2 \cong \Delta_p^3 \sum_{m,n} \sum_{\varepsilon\, S} (m^2 + n^2)^{\frac{1}{2}} p_{rq}(m\Delta_p, n\Delta_p) . \qquad (59)$$

One final nuance is that since region S can encompass negative values for m and/or n, whereas (56) is typically evaluated only for $0 \le m,n \le N-1$, the lookup for the appropriate value of $p_{rq}(m\Delta_p, n\Delta_p)$ to use with $(m^2 + n^2)^{\frac{1}{2}}$ in (59) is in bins

m modulo N and n modulo N, respectively. A program that achieves all of these features is listed in the appendix; it includes some diagnostic plots that keep track of the aliasing and attempt to control the error inherent in (59).

An example for K = 1, $R_x = R_y = 10$ yielded $\mu_1/(\sigma_x\sigma_y) = D_2 = 21.026487893$, when done exactly by means of (41). As an illustration of the accuracy of (59), it yielded $D_2 \cong 21.026487800$ for the same parameter values, using increment $\Delta_f = .06$ and N = 128. Also, $K_m = 200$ samples of characteristic function $f_{rq}(i\xi,i\eta)$ in each dimension were used, thereby minimizing termination error.

Another check on the above procedure and program was accomplished by deliberately taking, as a test case, a Gaussian two-dimensional characteristic function, and subjecting it to the above numerical techniques. The exact answer for the mean magnitude is furnished by (30) for this Gaussian example. In particular, for K = 10, $R_x = R_y = 1$, (30) yielded $\mu_{1g}/(\sigma_x\sigma_y) = 2.1577687$. On the other hand, for $\Delta_f = .6$, N = 128, $K_m = 50$, numerical procedure (59) yielded 2.1577675, an error of 1.2E-6.

DEFLECTION OF MAGNITUDE |G|, ANY K

We now have the ability to exactly evaluate the deflection d_c of magnitude estimate |G| defined in (35), and to compare it with the Gaussian approximation defined in (36) and evaluated in (37). A numerical comparison is presented in the table below.

Tabulation of Exact and Gaussian Deflections

K	R_x	R_y	μ_1	μ_{1g}	d_c	d_g	Δ_f	K_m
10	.5	.5	1.2131	1.2241	2.1558	2.2650	.5	50
10	1	.5	1.5978	1.6068	3.4135	3.5712	.5	50
10	1	1	2.1515	2.1578	5.2231	5.4517	.5	50
10	2	.5	2.1795	2.1859	5.3148	5.5477	.5	50
10	2	1	2.9701	2.9742	7.8990	8.2384	.5	50
10	2	2	4.1245	4.1272	11.672	12.174	.4	50
10	4	1	4.1505	4.1533	11.757	12.263	.3	50
10	4	4	8.1120	8.1133	24.706	25.779	.3	50
100	1	1	2.0150	2.0151	19.748	19.836	1.5	30

For K = 10, the agreement of mean magnitude μ_1 and Gaussian approximation μ_{1g} is very good over the entire range of parameter values considered, with the Gaussian approximation being a slight overestimate by less than 1%. On the other hand, the agreement between deflections d_c and d_g is not quite as good, with the Gaussian case overestimating by about 4.5%. High accuracy in the deflection for K = 10 can only be achieved through the detailed numerical procedure presented above; the Gaussian approximation has some limitations at this low value of K, the number of independent pieces.

On the other hand, for K = 100, the means are virtually identical, while the deflections differ by 0.5%. This is an illustration of the approach of summation variables R and Q in (7) to Gaussian for large numbers of pieces, K.

AUTO SPECTRUM ESTIMATE

In this section, we consider adding the two received processes together and estimating the resulting auto spectrum. We then evaluate the deflection of this auto spectrum estimate and compare it with the deflection for the magnitude of the complex cross spectrum estimate, $|G|$.

Since the two input noises $x(t)$ and $y(t)$ utilized in (6) and (7) can have different levels, we scale them and sum according to

$$z(t) = [s(t) + x(t)] + \lambda[s(t) + y(t)] =$$

$$= (1 + \lambda)\, s(t) + x(t) + \lambda\, y(t) \ . \qquad (60)$$

Scale factor λ will be chosen to maximize the deflection of the auto spectrum estimate of process $z(t)$. (More generally, we should filter the two processes and add.)

CHARACTERISTIC FUNCTION OF AUTO SPECTRUM ESTIMATE

Analogous to (4), (5), and (6), the k-th voltage density estimate, at analysis frequency f, of process $z(t)$ is

$$Z_k \equiv \int dt\, \exp(-i2\pi ft)\, w_k(t)\, z(t) =$$

$$= (1 + \lambda)\, \frac{A}{2}\, e^{i\phi}\, W_k(f-f_o) + X_k + \lambda\, Y_k =$$

$$= (1 + \lambda)(\alpha_k + i\beta_k) + a_k + ib_k + \lambda(c_k + id_k) \ . \qquad (61)$$

The auto spectrum estimate at analysis frequency f is given by

$$G_z \equiv \frac{1}{K}\sum_{k=1}^{K} |z_k|^2 = \frac{1}{K}\sum_{k=1}^{K} |(1+\lambda)(\alpha_k + i\beta_k) + e_k + if_k|^2 \ , \quad (62)$$

where independent Gaussian random variables

$$e_k \equiv a_k + \lambda\, c_k \ , \quad f_k \equiv b_k + \lambda\, d_k \ , \quad (63)$$

with properties

$$\overline{e_k} = 0 \ , \quad \overline{f_k} = 0 \ , \quad \overline{e_k^2} = \overline{f_k^2} = \sigma_x^2 + \lambda^2\,\sigma_y^2 \equiv \sigma_e^2 \ . \quad (64)$$

Here, we used (12) and (13). An alternative form for (62) is

$$G_z = \frac{1}{K}\sum_{k=1}^{K} \left[\left((1+\lambda)\,\alpha_k + e_k\right)^2 + \left((1+\lambda)\,\beta_k + f_k\right)^2\right] \ . \quad (65)$$

We now hold the set of random variables $\{\alpha_k\}$ and $\{\beta_k\}$ fixed and compute the conditional characteristic function of the k-th term of (65). Using (64), the Gaussian property of the random variables $\{e_k\}$ and $\{f_k\}$, and (17), the desired quantity is

$$F_k(i\xi) \equiv \overline{\exp\left[i\xi\left((1+\lambda)\alpha_k + e_k\right)^2 + i\xi\left((1+\lambda)\beta_k + f_k\right)^2\right]} =$$

$$= \iint de\, df\, \frac{1}{2\pi\sigma_e^2} \exp\left[-\frac{e^2+f^2}{2\sigma_e^2} + i\xi\left((1+\lambda)\alpha_k+e\right)^2 + i\xi\left((1+\lambda)\beta_k+f\right)^2\right] =$$

$$= \frac{1}{1 - i\xi 2\sigma_e^2} \exp\left(\frac{i\xi\,(1+\lambda)^2\,(\alpha_k^2+\beta_k^2)}{1 - i\xi 2\sigma_e^2}\right) \ . \quad (66)$$

But, by use of (9), the end result in (66) is not a random variable at all, and furthermore, does not depend on k. Therefore, the characteristic function of auto spectrum estimate G_z in (65) is given by

$$F(i\xi) = F_1\left(\frac{i\xi}{K}\right)^K = \left(1 - i\xi 2\sigma_e^2/K\right)^{-K} \exp\left(\frac{i\xi\ (1 + \lambda)^2\ \gamma}{1 - i\xi 2\sigma_e^2/K}\right) . \quad (67)$$

This result in (67) is exact. By expanding ln $F(i\xi)$ in a power series in $i\xi$, the j-th cumulant of estimate G_z is found to be

$$\chi_j = \frac{(j-1)!}{K^{j-1}} \left(2\sigma_e^2\right)^j \left[1 + j\frac{(1 + \lambda)^2\ R_x\ R_y}{\lambda^2\ R_x + R_y}\right] \quad \text{for } j \geq 1 , \quad (68)$$

where we used (64) and (22).

DISTRIBUTION OF AUTO SPECTRUM ESTIMATE

The exceedance distribution function corresponding to characteristic function (67) is the detection probability for random variable G_z and is given by [5]

$$P_d = Pr(G_z > v) = Q_K\left(\left(\frac{2K\ (1 + \lambda)^2\ R_x\ R_y}{\lambda^2\ R_x + R_y}\right)^{\frac{1}{2}}, \left(\frac{K\ v}{\sigma_x^2 + \lambda^2\ \sigma_y^2}\right)^{\frac{1}{2}}\right) , \quad (69)$$

where we used (64) and (22). The false alarm probability is obtained by setting $R_x = R_y = 0$, thereby yielding

$$P_f = \exp\left(-\frac{Kv/2}{\sigma_x^2 + \lambda^2 \sigma_y^2}\right) . \tag{70}$$

We now want to choose scale factor λ in (60) so as to maximize the detection probability while holding the false alarm probability fixed. This latter requirement means holding the argument of the exponential in (70) fixed, which makes threshold v a function of λ. It also makes the second argument of the Q_K function in (69) constant. Therefore, maximization of P_d is achieved by maximizing the first argument in (69), or equivalently by maximizing the quantity

$$\frac{(1 + \lambda)^2}{\lambda^2 R_x + R_y} \tag{71}$$

by choice of scale factor λ. The best choice is

$$\lambda = \frac{R_y}{R_x} , \tag{72}$$

leading to maximum value $1/R_x + 1/R_y$ for (71). Substitution of these results in (69) yield the maximum detection probability as

$$P_d = Q_K\left(\left(2K\ (R_x + R_y)\right)^{\frac{1}{2}}, \left(\frac{K\ v}{\sigma_x^2 + \sigma_y^2}\right)^{\frac{1}{2}} \frac{\sigma_y}{\sigma_x}\right) . \tag{73}$$

(The nonsymmetry in the second argument can be eliminated by using the symmetric combination $\eta[s(t) + x(t)]/\sigma_x + \eta^{-1}[s(t) + y(t)]/\sigma_y$ instead of (60), and choosing η optimally.) The corresponding false alarm probability is obtained by replacing the first argument in (73) by zero, that is, $R_x = R_y = 0$.

DEFLECTION OF AUTO SPECTRUM ESTIMATE

The deflection of auto spectrum estimate G_z is defined analogously to that for magnitude cross spectrum estimate $|G|$ in (35), namely

$$d_a \equiv \frac{\chi_1 - \chi_1(A=0)}{\chi_2(A=0)^{\frac{1}{2}}} = K^{\frac{1}{2}} \frac{(1+\lambda)^2 R_x R_y}{\lambda^2 R_x + R_y} , \tag{74}$$

where we used the relevant cumulants in (68). But, this quantity has exactly the same dependence on scale factor λ as does (71). Therefore the best choice of λ is again (72), leading to the maximum deflection, which is exact for all K, of

$$d_a = K^{\frac{1}{2}} (R_x + R_y) . \tag{75}$$

Thus, the choices of λ that maximize the deflection and the detection probability coincide for the auto spectrum estimate.

The maximum deflection d_a in (75) is not always larger than the magnitude cross spectrum deflection d_c considered earlier, even though (75) has utilized the best scale factor λ in summation (60). For example, for large K, we have from (38) the very good approximation,

$$d_g \sim K^{\frac{1}{2}} \left(\frac{4}{4-\pi} R_x R_y\right)^{\frac{1}{2}} \quad \text{as } K \to \infty . \tag{76}$$

The ratio of deflections is therefore given by

$$\frac{d_a}{d_g} \sim \left(\frac{4-\pi}{4}\right)^{\frac{1}{2}} \frac{R_x + R_y}{R_x^{\frac{1}{2}} R_y^{\frac{1}{2}}} = .463\left(\left(\frac{R_x}{R_y}\right)^{\frac{1}{2}} + \left(\frac{R_y}{R_x}\right)^{\frac{1}{2}}\right) \quad \text{as } K \to \infty . \tag{77}$$

The minimum value of this ratio is .926, reached when $R_y = R_x$. However, if $R_y/R_x > 2.207$ or if $R_y/R_x < .453$, then ratio (77) is always larger than 1. Thus, which deflection is larger (for large K) depends on the ratio $R_y/R_x = \sigma_x^2/\sigma_y^2$. For small K, direct numerical evaluation reveals that d_a is usually larger than d_c.

GRAPHICAL COMPARISON OF DEFLECTIONS

It was demonstrated in the previous section that the Gaussian approximation is rather accurate for evaluating the deflection of the magnitude cross spectrum estimate $|G|$, when K is larger than 10. The resulting Gaussian deflection d_g was given by (37) along with (29). On the other hand, the deflection d_a for the auto spectrum estimate G_z is given exactly by (75), and is valid for all K.

Plots of deflections d_g and d_a are presented in figures 1 and 2 for $R_y/R_x = 1$ and 1/2, respectively. They confirm the general behavior predicted earlier. For example, figure 1 for $R_y = R_x$ shows d_g to be larger than d_a for large K, but the curves cross for smaller values of K. On the other hand, figure 2 for $R_y = R_x/2$ has d_a generally larger than d_g, except when K gets very large. The ratio $R_y/R_x = 1/2$ is not smaller than the breakpoint .453 (above) that would guarantee d_a greater than d_g for large K.

The fact that cross spectrum deflection d_g (or d_c) is greater than auto spectrum deflection d_a for some ranges of the parameter

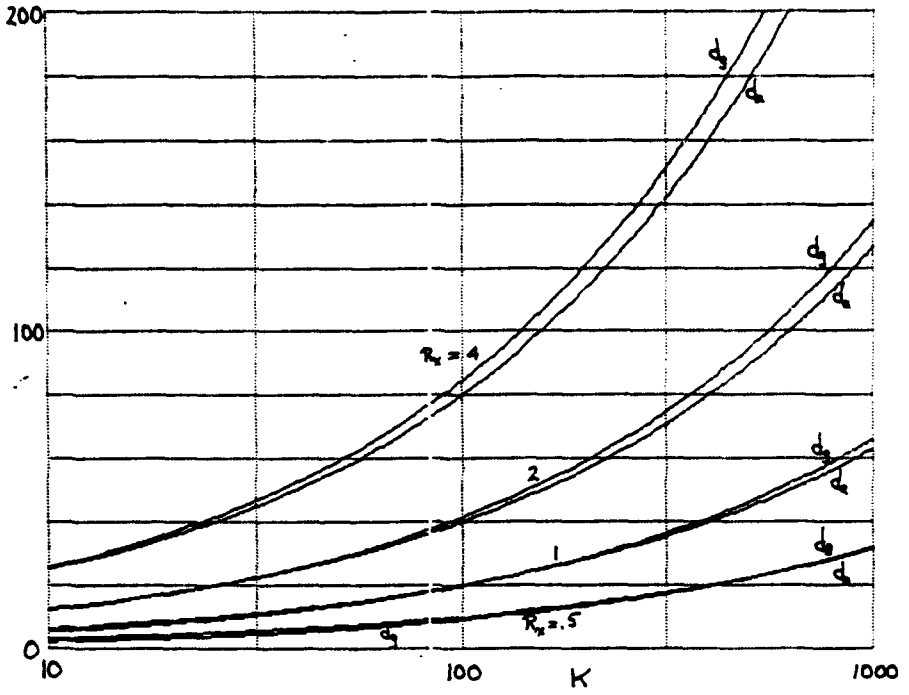

Figure 1. Deflections d_g and d_a for $R_y = R_x$

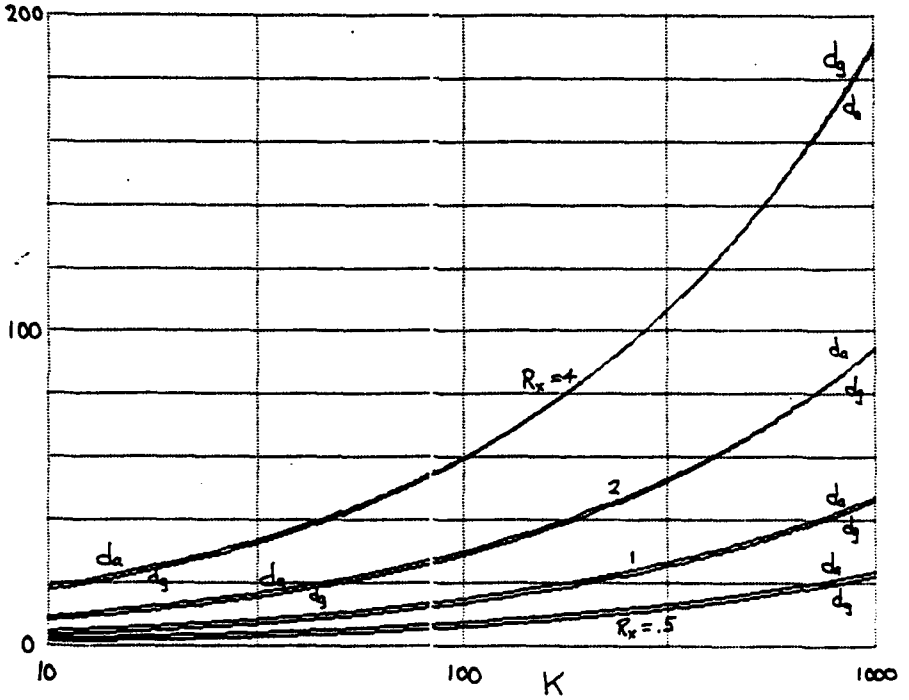

Figure 2. Deflections d_g and d_a for $R_y = R_x/2$

values does not necessarily reflect in the relative detection capability of the two processing techniques. After all, the deflection criterion only involves moments up through second order, whereas the full detection and false alarm probabilities involve all orders of moments. An example where the deflection of a random variable can be artificially accentuated is illustrated in the next section.

ACCENTUATION OF DEFLECTION

The deflection of a random variable is based upon its two lowest order moments, and can therefore be a misleading statistic regarding detectability. That is, the detection and false alarm probabilities depend on the entire probability density functions for signal present and absent, respectively, not just their first two moments.

To illustrate these points, consider detection of a Gaussian random variable x with mean m_0 under signal-absent hypothesis H_0, and mean m_1 ($> m_0$) under signal-present hypothesis H_1. Also, let the standard deviations have a common value σ under both hypotheses. Then, the deflection of random variable x is

$$d_x = \frac{m_1 - m_0}{\sigma} . \tag{78}$$

The detection probability, for threshold v, is given by

$$P_d = Pr(x > v|H_1) = \int_v^\infty \frac{du}{(2\pi)^{\frac{1}{2}}\sigma} \exp\left[-\frac{(u - m_1)^2}{2\sigma^2}\right] =$$

$$= \int_{(v-m_1)/\sigma}^\infty dt\ (2\pi)^{-\frac{1}{2}} \exp(-t^2/2) \equiv \Phi\left(\frac{m_1-v}{\sigma}\right) . \tag{79}$$

Similarly, the false alarm probability is given by

$$P_f = Pr(x > v|H_0) = \Phi\left(\frac{m_0-v}{\sigma}\right) . \tag{80}$$

For a given false alarm probability P_f, (80) can be solved for

threshold v, and then substituted into (79). The result is

$$P_d = \Phi\left(d_x + \tilde{\Phi}(P_f)\right) , \tag{81}$$

where $\tilde{\Phi}$ is the inverse Φ function, and we used (78). Thus, given a specified performance level P_f, P_d, the single parameter d_x completely quantifies performance. Observe that we are still using the entire probability density functions of x under H_0 and H_1, as we must in order to evaluate the exceedance distribution functions in (79) and (80); however, the receiver operating characteristic depends on only the single parameter d_x, through rule (81).

Now, let us consider a monotonic nonlinear distortion of random variable x, yielding new random variable y according to

$$y = \exp\left(C\frac{x}{\sigma}\right) , \tag{82}$$

where scaling C (> 0) is an unspecified constant at the moment. Obviously, the receiver operating characteristic for random variable y will be identical with that determined for x above in (79), (80), and (81); only the thresholds will change.

However, let us now consider the deflection of random variable y. Since x is Gaussian, we have under hypothesis H_k, the n-th moment of y in the form

$$\overline{y^n} = \overline{\exp\left(nC\frac{x}{\sigma}\right)} = \int \frac{du}{(2\pi)^{\frac{1}{2}}\sigma} \exp\left(-\frac{(u - m_k)^2}{2\sigma^2} + nC\frac{u}{\sigma}\right) =$$

$$= \exp\left(nC\frac{m_k}{\sigma} + \frac{1}{2}n^2C^2\right) . \tag{83}$$

The deflection of random variable y follows immediately as

$$d_y = \frac{\exp(Cd_x) - 1}{\left(\exp(C^2) - 1\right)^{\frac{1}{2}}} . \tag{84}$$

Deflection d_y depends on d_x and the dimensionless scaling C. If scaling C is very small, then we have $d_y \cong d_x$; this agrees with the observation that distortion (82) is virtually linear then.

However, if parameter C is substantial, deflection d_y can be <u>much</u> greater than d_x. In fact, given a value of d_x, there is a value of C, namely $C = d_x$, at which d_y peaks, with value

$$\max_C d_y = \left(\exp(d_x^2) - 1\right)^{\frac{1}{2}} . \tag{85}$$

As an example, the value of d_y is greater than 1000 if $d_x > 3.72$. Thus, the deflection of random variable y can be greatly accentuated relative to the deflection of x, merely by performing a monotonic nonlinear distortion. The ability to achieve this artificial improvement in deflection strongly cautions against relying on the deflection as a reliable measure of detectability.

SUMMARY

The joint characteristic function of the real and imaginary parts of the complex cross spectrum estimate has been derived in closed form, for arbitrary signal strength and noise spectra. For noise-only, the corresponding joint probability density function has also been derived in closed form and used to obtain exact results for fractional moments of the magnitude of the cross spectrum estimate. For signal present, an efficient two-dimensional fast Fourier transform numerical procedure has been utilized to get accurate probability density functions and moments.

When the number of pieces, K, used in the estimate of the cross spectrum is large, a Gaussian approximation has been employed for the joint probability density function of the real and imaginary parts. Numerical computations reveal that this Gaussian approximation is adequate if $K > 10$, and is very accurate for $K > 100$. This Gaussian approximation has then been used to determine the deflection of the magnitude of the cross spectrum estimate.

Comparisons of the deflections for the magnitude of the cross spectrum estimate and for the auto spectrum estimate reveal that they are rather close to each other. However, even though one deflection may be larger than the other for some ranges of parameter values, that does not necessarily make the corresponding processor a better detector. An example is presented to show how the deflection may be artificially enhanced

merely by nonlinear transformation of the decision variable, but without any change in the fundamental detectability of the signal.

A program is furnished in BASIC which enables calculation of the joint probability density function of the real and imaginary parts of the cross spectrum estimate, for arbitrary signal strength. In addition, it calculates the mean magnitude of the cross spectrum estimate and compares it with the Gaussian approximation.

APPENDIX - PROGRAM FOR CALCULATION OF μ_1

This appendix contains a listing of a BASIC program for the evaluation of the aliased joint probability density function p_{rq} given by (56), in addition to the normalized moment D_2 defined by (59). Inputs required of the user are Delf (Δ_f) in line 10, P (K) in line 20, Rx (R_x) in line 30, Ry (R_y) in line 40, N (N) in line 50, and Km (K_m) in line 60. An explanation of each of these symbols is given in the program listing.

The first plot produced is a slice of the magnitude of the aliased characteristic function $f_a(i\xi,i\eta)$ in (56) along the ξ axis; this affords a determination of whether adequate decay has been realized. The next plot displays the real and imaginary parts of f_a; this indicates whether the sampling rate is adequate to track the variations in these two functions.

Then, the sum of the sampled probability density function is computed and subtracted from 1; this error furnished a measure of the accuracy with which the density has been calculated. Next, a slice of density $p(u,v)$ along the u axis is plotted; this indicates whether sufficient decay has been achieved before the aliasing shows up. (Strictly, this observation replaces the one above on the real and imaginary parts of f_a.) The user must also note the maximum location of the density and enter this number into the program at this point. Finally, a slice of $p(u,v)$ in v, for u equal to the maximum location, is plotted; this guarantees that adequate decay in the other dimension of the density has been achieved.

The values of μ_1, μ_{1g}, $\mu_1(A=0)$, d_c, and d_g are then printed out. This complete procedure furnishes a measure of accuracy of the Gaussian approximation results, provided that sufficient decays have been realized in all the plots indicated above.

```
 10    Delf=.5          !  INCREMENT FOR CHARACTERISTIC FUNCTION
 20    P=10.            !  NUMBER OF PIECES, K
 30    Rx=1.            !  MEASURE OF SIGNAL-TO-NOISE RATIO IN x
 40    Ry=1.            !  MEASURE OF SIGNAL-TO-NOISE RATIO IN y
 50    N=128            !  SIZE OF FAST FOURIER TRANSFORM
 60    Km=50            !  NUMBER OF SAMPLES IN EACH DIMENSION
 70    DOUBLE N,Km,N1,K,L,Kt,Lt,K1   !  INTEGERS
 80    DIM Fr(127,127),Fi(127,127),X(127),Y(127),Cos(32)
 90    N1=N-1
100    REDIM Fr(0:N1,0:N1),Fi(0:N1,0:N1),X(0:N1),Y(0:N1),Cos(0:N/4)
110    T1=Delf*Delf/(P*P)
120    T2=(Rx+Ry)*Delf*Delf/P
130    T3=2.*SQR(Rx*Ry)*Delf
140    A=2.*PI/N
150    FOR K=0 TO N/4
160    Cos(K)=COS(A*K)      !  QUARTER-COSINE TABLE IN Cos(*)
170    NEXT K
180    FOR K=0 TO Km
190    Kt=K MODULO N
200    K2=K*K
210    T4=T3*K
220    FOR L=-Km TO Km
230    Lt=L MODULO N
240    Sq=K2+L*L
250    T=1.+T1*Sq
260    A=-P*LOG(T)-T2*Sq/T
270    IF A<-500. THEN 320
280    E=EXP(A)
290    A=T4/T
300    Fr(Kt,Lt)=Fr(Kt,Lt)+E*COS(A)   !  COLLAPSING
310    Fi(Kt,Lt)=Fi(Kt,Lt)+E*SIN(A)
320    NEXT L
330    NEXT K
340    GINIT
350    GRAPHICS ON
360    WINDOW 0,N,-10,0
370    GRID N/8,1
380    FOR K=0 TO N1
390    Fr=Fr(K,0)
400    Fi=Fi(K,0)
410    Fs=Fr*Fr+Fi*Fi
420    IF Fs>0. THEN 450
430    PENUP
440    GOTO 460
450    PLOT K,LGT(Fs)*.5
460    NEXT K
470    PENUP
480    PRINT "          |f(xi,0)|"
490    PAUSE
500    PRINT "          Re f(xi,0)  and  Im f(xi,0)"
```

```
510     GCLEAR
520     WINDOW 0,N,-1,1
530     GRID N/8,.2
540     FOR K=0 TO N1
550     PLOT K,Fr(K,0)   !  Re f(xi,0)
560     NEXT K
570     PENUP
580     LINE TYPE 3
590     FOR K=0 TO N1
600     PLOT K,Fi(K,0)   !  Im f(xi,0)
610     NEXT K
620     PENUP
630     LINE TYPE 1
640     FOR K=0 TO N1
650     FOR L=0 TO N1
660     X(L)=Fr(K,L)
670     Y(L)=Fi(K,L)
680     NEXT L
690     IF K>0 THEN 720
700     MAT X=X*(.5)
710     MAT Y=Y*(.5)
720     CALL Fft14(N,Cos(*),X(*),Y(*))
730     FOR L=0 TO N1
740     Fr(K,L)=X(L)
750     Fi(K,L)=Y(L)
760     NEXT L
770     NEXT K
780     FOR L=0 TO N1
790     FOR K=0 TO N1
800     X(K)=Fr(K,L)
810     Y(K)=Fi(K,L)
820     NEXT K
830     CALL Fft14(N,Cos(*),X(*),Y(*))
840     FOR K=0 TO N1
850     Fr(K,L)=X(K)
860   ! Fi(K,L)=Y(K)    !  Fi(*) unnecessary
870     NEXT K
880     NEXT L
890     MAT Fr=Fr*(Delf*Delf/(2.*PI*PI))
900     Delp=2.*PI/(N*Delf)
910     S=SUM(Fr)*Delp*Delp
920     PRINT "P =";P;"     Rx =';Rx;"     Ry =";Ry
930     PRINT "ERROR =";S-1.
940     PRINT "          p(u,0)"
950     GCLEAR
960     WINDOW 0,N,-12,0
970     GRID N/8,1
980     FOR K=0 TO N1
990     Fr=Fr(K,0)
1000    IF Fr<>0. THEN 1030
1010    PENUP
1020    GOTO 1040
1030    PLOT K,LGT(ABS(Fr))
1040    NEXT K
1050    PLOT N,LGT(Fr(0,0))
1060    PENUP
1070    INPUT "MAXIMUM LOCATION OF Fr(K,0):",K1
1080    PRINT "          p(u1,v)'
1090    GCLEAR
1100    WINDOW 0,N,-12,0
```

```
1110    GRID N/8,1
1120    FOR L=0 TO N1
1130    Fr=Fr(K1,L)
1140    IF Fr<>0. THEN 1170
1150    PENUP
1160    GOTO 1180
1170    PLOT L,LGT(ABS(Fr))
1180    NEXT L
1190    PLOT N,LGT(Fr(K1,0))
1200    PENUP
1210    PAUSE
1220    GCLEAR
1230    M1=0.
1240    FOR K=K1-N/2 TO K1+N/2
1250    Kt=K MODULO N
1260    K2=K*K
1270    FOR L=-N/2 TO N/2
1280    Lt=L MODULO N
1290    M1=M1+SQR(K2+L*L)*Fr(Kt,Lt)
1300    NEXT L
1310    NEXT K
1320    M1=M1*Delp*Delp*Delp
1330    PRINT "        Mu1 =";M1
1340    V=P*Rx*Ry/(1.+Rx+Ry)
1350    CALL F11(-.5,1.,-V,F11,I)
1360    M1g=SQR(PI*(1.+Rx+Ry)/P)*F11
1370    PRINT "Mu1(GAUSS) =";M1g
1380    M10=PI
1390    FOR K=1 TO P
1400    M10=M10*(K-.5)/K
1410    NEXT K
1420    PRINT "Mu1(0) =";M10
1430    M2=4./P
1440    Dc=(M1-M10)/SQR(M2-M10*M10)
1450    PRINT "        Dc =";Dc
1460    Dg=SQR(PI/(4.-PI))*(SQR(1.+Rx+Ry)*F11-1.)
1470    PRINT "Dc(GAUSS) =";Dg
1480    PRINT
1490    PAUSE
1500    END
1510    !
1520    SUB Fft14(DOUBLE N,REAL Cos(*),X(*),Y(*)) ! N<=2^14=16384; 0 SUBS
1530    DOUBLE Log2n,N1,N2,N3,N4,J,K   !  INTEGERS < 2^31 = 2,147,483,648
1540    DOUBLE I1,I2,I3,I4,I5,I6,I7,I8,I9,I10,I11,I12,I13,I14,L(0:13)
1550    IF N=1 THEN SUBEXIT
1560    IF N>2 THEN 1640
1570    A=X(0)+X(1)
1580    X(1)=X(0)-X(1)
1590    X(0)=A
1600    A=Y(0)+Y(1)
1610    Y(1)=Y(0)-Y(1)
1620    Y(0)=A
1630    SUBEXIT
1640    A=LOG(N)/LOG(2.)
1650    Log2n=A
```

```
1660    IF ABS(A-Log2n)<1.E-8 THEN 1690
1670    PRINT "N =";N;"IS NOT A POWER OF 2; DISALLOWED."
1680    PAUSE
1690    N1=N/4
1700    N2=N1+1
1710    N3=N2+1
1720    N4=N3+N1
1730    FOR I1=1 TO Log2n
1740    I2=2^(Log2n-I1)
1750    I3=2*I2
1760    I4=N/I3
1770    FOR I5=1 TO I2
1780    I6=(I5-1)*I4+1
1790    IF I6<=N2 THEN 1830
1800    A1=-Cos(N4-I6-1)
1810    A2=-Cos(I6-N1-1)
1820    GOTO 1850
1830    A1=Cos(I6-1)
1840    A2=-Cos(N3-I6-1)
1850    FOR I7=0 TO N-I3 STEP I3
1860    I8=I7+I5-1
1870    I9=I8+I2
1880    T1=X(I8)
1890    T2=X(I9)
1900    T3=Y(I8)
1910    T4=Y(I9)
1920    A3=T1-T2
1930    A4=T3-T4
1940    X(I8)=T1+T2
1950    Y(I8)=T3+T4
1960    X(I9)=A1*A3-A2*A4
1970    Y(I9)=A1*A4+A2*A3
1980    NEXT I7
1990    NEXT I5
2000    NEXT I1
2010    I1=Log2n+1
2020    FOR I2=1 TO 14
2030    L(I2-1)=1
2040    IF I2>Log2n THEN 2060
2050    L(I2-1)=2^(I1-I2)
2060    NEXT I2
2070    K=0
2080    FOR I1=1 TO L(13)
2090    FOR I2=I1 TO L(12) STEP L(13)
2100    FOR I3=I2 TO L(11) STEP L(12)
2110    FOR I4=I3 TO L(10) STEP L(11)
2120    FOR I5=I4 TO L(9) STEP L(10)
2130    FOR I6=I5 TO L(8) STEP L(9)
2140    FOR I7=I6 TO L(7) STEP L(8)
2150    FOR I8=I7 TO L(6) STEP L(7)
2160    FOR I9=I8 TO L(5) STEP L(6)
2170    FOR I10=I9 TO L(4) STEP L(5)
2180    FOR I11=I10 TO L(3) STEP L(4)
2190    FOR I12=I11 TO L(2) STEP L(3)
2200    FOR I13=I12 TO L(1) STEP L(2)
```

```
2210    FOR I14=I13 TO L(0) STEP L(1)
2220    J=I14-1
2230    IF K>J THEN 2300
2240    A=X(K)
2250    X(K)=X(J)
2260    X(J)=A
2270    A=Y(K)
2280    Y(K)=Y(J)
2290    Y(J)=A
2300    K=K+1
2310    NEXT I14
2320    NEXT I13
2330    NEXT I12
2340    NEXT I11
2350    NEXT I10
2360    NEXT I9
2370    NEXT I8
2380    NEXT I7
2390    NEXT I6
2400    NEXT I5
2410    NEXT I4
2420    NEXT I3
2430    NEXT I2
2440    NEXT I1
2450    SUBEND
2460    !
2470    SUB F11(A,B,X,F11,D)     !  POWER SERIES
2480    Error=1.E-16             !  RELATIVE ERROR TOLERANCE
2490    Number=1000              !  MAXIMUM NUMBER OF TERMS IN SERIES
2500    DOUBLE Number,N          !  INTEGERS
2510    B1=B-1.
2520    IF X<0. THEN 2640
2530    A1=A-1.
2540    F11=T=Big=1.
2550    FOR N=1 TO Number
2560    Fn=FLT(N)
2570    T=T*X*(Fn+A1)/(Fn*(Fn+B1))
2580    F11=F11+T
2590    Af=ABS(F11)
2600    Big=MAX(Big,Af)
2610    IF ABS(T)<=Error*Af THEN 2750
2620    NEXT N
2630    GOTO 2740
2640    Ba1=B-A-1.
2650    F11=T=Big=EXP(X)
2660    FOR N=1 TO Number
2670    Fn=FLT(N)
2680    T=-T*X*(Fn+Ba1)/(Fn*(Fn+B1))
2690    F11=F11+T
2700    Af=ABS(F11)
2710    Big=MAX(Big,Af)
2720    IF ABS(T)<=Error*Af THEN 2750
2730    NEXT N
2740    PRINT Number;"TERMS IN SUB F11 AT ";A;B;X
2750    D=15.-LGT(Big/Af)        !  NUMBER OF SIGNIFICANT DIGITS
2760    SUBEND
```

REFERENCES

[1] A. H. Nuttall, **Estimation of Cross-Spectra via Overlapped Fast Fourier Transform Processing**, NUSC Technical Report 4169-S, Naval Underwater Systems Center, New London, CT, 11 July 1975.

[2] I. S. Gradshteyn and I. M. Ryzhik, **Table of Integrals, Series, and Products**, Academic Press, Inc., New York, NY, 1980.

[3] **Handbook of Mathematical Functions**, U. S. Department of Commerce, National Bureau of Standards, Applied Mathematics Series, number 55, U. S. Government Printing Office, Washington, DC, June 1964.

[4] D. Middleton, **An Introduction to Statistical Communication Theory**, McGraw-Hill Book Company, Inc., New York, NY, 1960.

[5] A. H. Nuttall, **Some Integrals Involving the Q_M-Function**, NUSC Technical Report 4755, Naval Underwater Systems Center, New London, CT, 15 May 1974.

Reverse Blank

INITIAL DISTRIBUTION LIST

Addressee	Number of Copies
Center for Naval Analyses, VA	1
Coast Guard Academy, CT	
J. Wolcin	1
Defense Technical Information Center, VA	12
Griffiss Air Force Base, NY	
Documents Library	1
J. Michels	1
National Radio Astronomy Observatory, VA	
F. Schwab	1
National Security Agency, MD	
J. Maar	1
National Technical Information Service, VA	10
Naval Air Warfare Center, PA	
Commander	1
L. Allen	1
T. Madera	1
Naval Command Control and Ocean Surveillance Center, CA	
Commanding Officer	1
J. Alsup	1
D. Hanna	1
W. Marsh	1
P. Nachtigall	1
C. Persons	1
C. Tran	1
Naval Environmental Prediction Research Facility, CA	1
Naval Intelligence Command, DC	1
Naval Oceanographic and Atmospheric Research Laboratory, CA	
M. Pastore	1
Naval Oceanographic and Atmospheric Research Laboratory, MS	
Commanding Officer	1
B. Adams	1
R. Fiddler	1
E. Franchi	1
R. Wagstaff	1
Naval Oceanographic Office, MS	1
Naval Personnel Research and Development Center, CA	1
Naval Postgraduate School, CA	
Superintendent	1
C. Therrien	1
Naval Research Laboratory, FL	1
Naval Research Laboratory, DC	
Commanding Officer	1
D. Bradley	1
W. Gabriel	1
A. Gerlach	1
D. Steiger	1
E. Wald	1
N. Yen	1

INITIAL DISTRIBUTION LIST (CONT'D)

Addressee	Number of Copies
Naval Sea Systems Command, DC	
SEA-00; -63; -63D; -63X; -92R; PMS-402	6
Naval Surface Warfare Center, FL	
Commanding Officer	1
E. Linsenmeyer	1
D. Skinner	1
Naval Surface Warfare Center, MD	
P. Prendergast	1
Naval Surface Warfare Center, VA	
J. Gray	1
Naval Surface Weapons Center, FL	1
Naval Surface Weapons Center, MD	
Officer in Charge	1
M. Strippling	1
Naval Surface Weapons Center, VA	
Commander	1
H. Crisp	1
D. Phillips	1
T. Ryczek	1
Naval Technical Intelligence Center, DC	
Commanding Officer	1
D. Rothenberger	1
Naval Undersea Warfare Center, FL	
Officer in Charge	1
R. Kennedy	1
Naval Weapons Center, CA	1
Office of the Chief of Naval Research, VA	
OCNR-00; -10; -11; -12; -13; -20; -21; -22; -23 (3)	11
P. Abraham	1
N. Gerr	1
D. Johnson	1
A. Wood	1
Space and Naval Warfare System Command, DC	
SPAWAR-00; -04; -005; PD-80; PMW-181	5
R. Cockerill	1
L. Parrish	1
U. S. Air Force, Maxwell Air Force Base, AL	
Air University Library	1
U. S. Department of Commerce, CO	
A. Spaulding	1
Vandenberg Air Force Base, CA	
R. Leonard	1